JOURNAL OF THE AMERICAN WATER RESOURCES ASSOCIATION
Vol. 45, No. 6 AMERICAN WATER RESOURCES ASSOCIATION December 2009

A CALIBRATED, HIGH-RESOLUTION GOES SATELLITE SOLAR INSOLATION PRODUCT FOR A CLIMATOLOGY OF FLORIDA EVAPOTRANSPIRATION[1]

Simon J. Paech, John R. Mecikalski, David M. Sumner, Chandra S. Pathak, Quinlong Wu, Shafiqul Islam, and Taiye Sangoyomi[2]

ABSTRACT: Estimates of incoming solar radiation (insolation) from Geostationary Operational Environmental Satellite observations have been produced for the state of Florida over a 10-year period (1995-2004). These insolation estimates were developed into well-calibrated half-hourly and daily integrated solar insolation fields over the state at 2 km resolution, in addition to a 2-week running minimum surface albedo product. Model results of the daily integrated insolation were compared with ground-based pyranometers, and as a result, the entire dataset was calibrated. This calibration was accomplished through a three-step process: (1) comparison with ground-based pyranometer measurements on clear (noncloudy) reference days, (2) correcting for a bias related to cloudiness, and (3) deriving a monthly bias correction factor. Precalibration results indicated good model performance, with a station-averaged model error of 2.2 MJ m^{-2}/day (13%). Calibration reduced errors to 1.7 MJ m^{-2}/day (10%), and also removed temporal-related, seasonal-related, and satellite sensor-related biases. The calibrated insolation dataset will subsequently be used by state of Florida Water Management Districts to produce statewide, 2-km resolution maps of estimated daily reference and potential evapotranspiration for water management-related activities.

(KEY TERMS: solar insolation; evapotranspiration; remote sensing; water resources management; reference evapotranspiration; Penman-Monteith.)

Paech, Simon J., John R. Mecikalski, David M. Sumner, Chandra S. Pathak, Quinlong Wu, Shafiqul Islam, and Taiye Sangoyomi, 2009. A Calibrated, High-Resolution GOES Satellite Solar Insolation Product for a Climatology of Florida Evapotranspiration. *Journal of the American Water Resources Association* (JAWRA) 45(6):1328-1342. DOI: 10.1111/j.1752-1688.2009.00366.x

INTRODUCTION

Estimates of incoming solar radiation (insolation) from satellite data for the state of Florida over a 10-year period (June 1, 1995 to December 31, 2004) have been produced for use by state of Florida Water Management Districts (WMD) for evapotranspiration (ET) estimation using a Penman-Monteith technique (Penman, 1948; Monteith, 1965). For producing reference ET, the Penman-Monteith relationship is used together with "crop coefficient" values. Solar insolation is the largest determinant for temporal variation in ET, which is a critical variable for water management, both in hydrologic flow simulations (involving potential ET) and water allocation and agricultural

[1]Paper No. JAWRA-08-0132-P of the *Journal of the American Water Resources Association* (JAWRA). Received July 7, 2008; accepted July 7, 2009.

[2]Respectively, Research Associate and Assistant Professor (Paech and Mecikalski), Department of Atmospheric Sciences, University of Alabama in Huntsville, Huntsville, Alabama; Hydrologist (Sumner), U.S. Geological Survey, Florida Integrated Science Center, Orlando, Florida; Principal Engineer, Senior Engineer, and Lead Engineer (Pathak, Wu, and Sangoyomi), Operations and Hydro Data Management Division, South Florida Water Management District, West Palm Beach, Florida; and Professor (Islam), Department of Civil and Environmental Engineering, Tufts University, Medford, Massachusetts (E-Mail/Paech: johnm@nsstc.uah.edu).

water use (involving reference ET). The most desirable ET datasets for these purposes are spatially continuous, rather than point values derived from traditional field station networks, thus statewide mapping of ET is greatly facilitated by satellite-derived estimates of the spatial distribution of solar insolation. To date, the five Florida WMD have not had access to a common source of solar insolation data or methodologies for calculating the two most widely used indicators of ET (potential and reference ET). The motivation of this work is to develop a robust insolation calibration framework coupled to a satellite-based insolation model, so to provide for key radiative datasets for the formulation of a 10-year long, ET climatology (which will extend indefinitely into the future). These insolation datasets are used in conjunction with other information, such as net radiation, soil heat flux, and temporally varying crop coefficients, in the formulation of ET. This paper focuses only on the development of the insolation data, and subsequent calibration activities, demonstrating the powerful utility of satellite-derived fields for water resource applications.

Applications of a high-resolution (≤5 km) solar insolation dataset include its use in the development of reference ET and potential ET. Reference ET is valuable for irrigation scheduling and water management, while potential ET can be used as input into surface and groundwater hydrological models, whereas the solar insolation data themselves may be used as boundary conditions in certain ecosystem models. Clearly, geostationary satellites provide spatially and temporally continuous data across all regions in their view (between approximately ±55° latitude), a huge advantage over ground-based instrumentation. Use of a satellite-based insolation algorithm also ensures that a consistent algorithm is applied across an entire region.

Satellite visible data have been used for estimating solar insolation for a number of years, with methods ranging from statistical-empirical relationships such as Tarpley (1979), to physical models of varying complexity (see Gautier *et al.*, 1980, 1984; Diak and Gautier, 1983; Möser and Raschke, 1984; Pinker and Ewing, 1985; Dedieu *et al.*, 1987; Darnell *et al.*, 1988; Frouin and Chertock, 1992; Pinker and Laszlo, 1992; Weymouth and LeMarshall, 1999). Studies such as Schmetz (1989) and Pinker *et al.* (1995) have proven the utility of satellite-estimated solar insolation methods, showing that such models produce fairly accurate results – with hourly insolation estimates within 5-10% of pyranometer data during clear-sky conditions (15-30% for all sky conditions) and daily estimates within 10-15%. Additional works such as those of Stewart *et al.* (1999) and Otkin *et al.* (2005) have further bolstered the utility of this technique. Advantages of using satellite-estimated insolation data over those collected by pyranometer networks include large spatial coverage; high spatial resolution; the availability of data in remote, inaccessible, or potentially hazardous regions, over oceans and large water bodies (e.g., Frouin *et al.*, 1988); and in countries that may not have the means to install a ground-based pyranometer network.

A similar effort to that developed here for estimating solar insolation from satellite is described by Cosgrove *et al.* (2003a,b). In these studies, use of the Global Energy and Water Cycle Experiment (GEWEX) Surface Radiation Budget (SRB) downward solar flux algorithm (Pinker and Laszlo, 1992) has been demonstrated within the North American Land Data Assimilation project. The error statistics for the SRB product are comparable to those shown via this study (see Model Calibration), while the resolution of the SRB solar flux data are 0.5° resolution (see Meng *et al.*, 2003). The main reason for not using SRB here is that the needed resolution deemed important for estimating ET over Florida was on or near the cumulus cloud scale, namely 1-3 km, far above that of SRB data. SRB data are developed from a combination of polar orbiting and geostationary satellite data, while the solar insolation fields described here are developed only from Geostationary Operational Environmental Satellite (GOES) data. A more thorough description of the GEWEX SRB data is available at http://www.gewex-srb.larc.nasa.gov.

Other limitations for much of this previous work have been centered around the need for information on atmospheric parameters that limit the effectiveness of these models, such as aerosols and precipitable water (PW) information. Problems associated with assessing the performance of these models are often fraught with issues related to scale differences between point observations and satellite pixel resolution (from ~1 to 4 km). Satellite sensor degradation, especially prevalent on the National Oceanic and Atmospheric Administration (NOAA) GOES satellite series, are often difficult to quantify, albeit it is one aspect this study attempts to address.

In this study, data from the NOAA GOES "East" series of satellites are used. GOES data were obtained from the GOES data archive at the Space Science and Engineering Center at the University of Wisconsin-Madison. Approximately 102,000 individual GOES images were processed for this effort. These data were processed using the model of Gautier *et al.* (1980) to produce half-hourly and daily integrated solar insolation and 2-week running minimum surface albedo data throughout the state of Florida at 2-km horizontal spatial resolution. As noted above, this high-resolution was chosen to provide solar insolation observations between cumulus

clouds, which comprise a significant component of Florida's cloud climatology.

The other unique aspect of this work involved an extensive model calibration activity for the insolation product, undertaken by comparing satellite-derived insolation estimates to that of ground-based pyranometers and clear-sky radiation models. This comparison provided information to tune or adjust biases in the daily integrated insolation dataset for local environmental conditions. This was achieved via a three-step process: (1) comparison with ground-based pyranometer measurements on clear (noncloudy) reference days, (2) correcting for a bias related to cloudiness, and (3) deriving a monthly bias correction factor. This resulted in a significant reduction in bias errors and henceforth the formation of a very robust ET product.

The goal of this paper is to describe the production and calibration of a 2 km GOES-based insolation product, for eventual applications related to water management and ET. The approach is deemed simple, and once bias corrections are determined, insolation data with good error statistics without need for ancillary datasets are the result. The paper proceeds as follows: The Solar Insolation Model section of this paper provides an overview of the insolation model; Data Acquisition, Processing, and Quality Control section discusses data acquisition, processing, and quality control; Model Calibration details the model calibration efforts; followed by Discussion of Calibration Issues; and Summary and Conclusion, respectively.

THE SOLAR INSOLATION MODEL

The model developed by Gautier *et al.* (1980) [with modifications by Diak and Gautier (1983) and updated application methods by Diak *et al.* (1996), from this point onwards referred to as the "GDM"] employs a fairly simple physical representation of cloud and atmosphere radiative processes, yet has been shown to perform as well as, or even better than, more complex methods over a variety of land-surface and climatic conditions (Gautier *et al.*, 1984; Raphael and Hay, 1984; Frouin *et al.*, 1988; Diak *et al.*, 1996; Jacobs *et al.*, 2002, 2004; Otkin *et al.*, 2005). When comparing with pyranometer data, these studies reported root mean square errors (RMSEs) in hourly and daily insolation estimates (as a percentage of the mean pyranometer observed value) from 17 to 28 and 9 to 10%, respectively. The high ends of these errors (~28 and ~10%, respectively) were reported in the study of Jacobs *et al.* (2002), which took place over northern-central Florida and was characterized by significant convective-cloud activity. The GDM has also been proven in operational use, producing near-real-time insolation estimates for regional-scale and continental-scale land-surface carbon and water flux assessments (Mecikalski *et al.*, 1999; Anderson *et al.*, 2003, 2004), subsurface hydrologic modeling, and the generation of agricultural forecasting products (Diak *et al.*, 1998; Anderson *et al.*, 2001). A full description of the GDM is given by Gautier *et al.* (1980), Diak and Gautier (1983), and Diak *et al.* (1996) – a basic overview is given here.

The model is based on conservation of radiant energy in the Earth-atmosphere column. The GDM has two modes for determining solar insolation received at the Earth's surface: one for clear and one for cloudy conditions, based on satellite-inferred surface albedo data. A running 2-week minimum of this albedo data, reassessed at solar noon daily, is stored for each GOES visible data pixel, yielding a reference albedo grid representative of clear-sky conditions and capturing temporal changes in land-surface characteristics. This approach represents the true land-surface albedo more accurately than using the daily estimated value because the latter can be corrupted by high albedo values when clouds are present during the course of a day. [It should be noted that this minimum albedo product is wavelength-specific, unique to the GOES visible sensor (which does in fact include contributions from the near infrared), and therefore does not represent a true surface albedo.]

Within the GDM, for a given GOES image, the digital brightness at each image pixel is compared to that of the stored clear-sky reference albedo data for that pixel. If the brightness exceeds a given threshold [a function of the 2-week running minimum noontime albedo; Diak and Gautier (1983)], the pixel is deemed cloudy, and *vice versa*. Based on this determination, either a clear or cloudy model of atmospheric radiation processes is used to calculate solar insolation received at the surface, for each pixel. Both the clear and cloudy models incorporate parameterizations for ozone absorption, Raleigh scattering, and water vapor absorption within the atmospheric column using simple bulk relationships – the use of fixed ozone and aerosol contents being sufficient given that these produce secondary, smaller sources of error. The cloudy GDM component estimates a cloud-top albedo, and accounts for atmospheric effects above and below the cloud separately.

For the water vapor absorption parameterization, a fixed, approximate annual median value of 3.0 cm was used to estimate atmospheric column-integrated PW during the initial processing. [PW is defined as the amount of water that would precipitate out of a

vertical column of the atmosphere if all the water vapor were condensed into liquid.] PW data are needed to calculate the slantwise path, and subsequently the absorption coefficients in the Gautier *et al.* (1980) method. Postprocessing adjustments were then made to account for diurnal variations of PW (i.e., PW values greater or less than the 3.0 cm median value), given the logistical difficulty of including these data within the modeling stage. These adjustments were made by deriving diurnal adjustment factors based on daily representative PW values over Florida from numerical weather prediction (NWP) model data [National Centers for Environmental Prediction reanalysis dataset (NOAA/OAR/ESRL PSD, Boulder, Colorado; http://www.cdc.noaa.gov)]. In many instances, daily PW values over Florida were well above 3.0 cm, certainly during summer, while wintertime values were often much lower. No accounting was made for daily variations in PW considering the relatively small amount of inter-day variability that typically occurs over Florida, especially during summer, and because this would have required a reliance on forecasts from these models, which are often incorrect. We also do not account for meso-γ scale (2-25 km) scale variations in PW given this would require substantially larger amounts of model-derived data. Data from NWP models would need to be incorporated if constructing similar insolation climatologies for regions outside Florida with very high daily variations in PW.

DATA ACQUISITION, PROCESSING, AND QUALITY CONTROL

GOES Satellite Data

The GOES East series of satellites (the most recent additions being GOES-8 and GOES-12) have been placed in geostationary orbit above the Earth's equator at longitude 75°W, providing continuous observations in several visible and nonvisible radiation bands of much of the western hemisphere at high spatial (≥1 km) and temporal (≥15 min) resolution, making data collected by them ideal for high-resolution estimates of solar insolation. During the time period spanned by this study, the GOES-8 satellite (launched in April 1994) was decommissioned and the GOES-12 satellite took its place on April 1, 2003. Data from both of these satellites were acquired and utilized.

Although the GOES visible sensors have a nadir (the point directly below the satellite) spatial resolution of 1 km, this resolution decreases the further from nadir the instrument scans: for the state of Florida region, the highest resolution attainable is about 1.5-2.0 km. This was the input and output resolution of the GDM in this work. Half-hourly solar insolation values were calculated using GOES data from 15 and 45 min past the hour, and daily values were calculated by integrating the half-hourly values over the period of daylight (using the trapezoidal integration method). A simple method for computing sunrise and sunset times per pixel across the domain was used. The running 2-week minimum albedo product discussed in the section The Solar Insolation Model was calculated using data at solar noon. These products were generated both in the original satellite projection, and translated to a grid identical to that used for the Statewide NEXRAD radar-derived rainfall estimation product (Hoblit *et al.*, 2003). In the latter dataset, the data were interpolated in time to 00 and 30 min past the hour.

Potential GOES data issues include sensor degradation with time and sun glint effects (i.e., the reflection of the Sun's disk from land and sea surfaces). The effects of the latter are small, and not addressed in this study due to the complexity of the phenomena. Sensor degradation is addressed and corrected for through the calibration of the product, detailed in following sections. This issue is also discussed further in the section titled Discussion of Calibration Issues.

In general, GOES satellite data are available on a continual basis with high reliability. Under specific conditions though, the instruments are shut down (for example when sunlight shines directly into the sensors), and other issues such as receiving-station glitches can result in the occasional loss or corruption of an image or series of images. For this reason, if more than five half-hourly satellite images were missing on a given day, the daily insolation value for that day (being derived from the half-hourly data) was flagged as unusable. Days with three to five missing images were designated usable, and those with zero to two missing images were designated as good quality data. Where there were gaps in the usable data, linear interpolation was used to fill them. (The final insolation product includes flags for data loss.)

Pyranometer Data

Pyranometer data used to calibrate the satellite isolation product, and subsequently assess calibration performance, were obtained from a number of weather stations networks across Florida, each maintained by a different agency. The state of Florida is divided into five regional WMDs: Northwest Florida (NWF), South Florida (SF), St. Johns River (SJR), Suwannee River (SR), and Southwest Florida (SWF) as shown in Figure 1. Historical pyranometer data

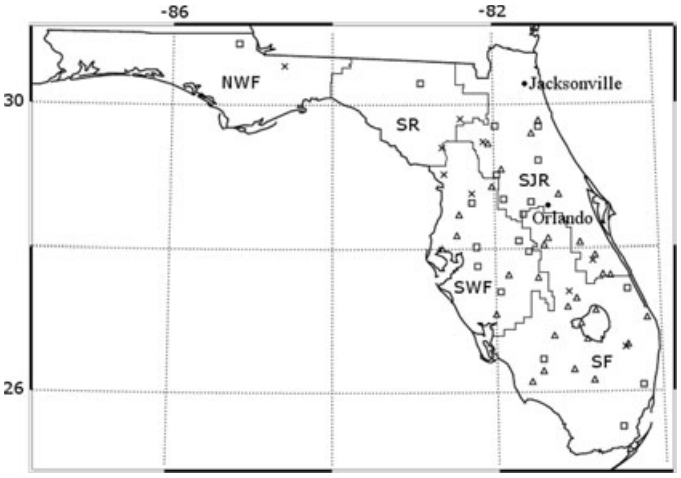

FIGURE 1. Locations of Pyranometer Stations Used in the Study. Groups 1, 2, and 3 datasets are denoted by crosses, triangles, and squares, respectively. State boundaries and WMD region boundaries are thick and thin black lines, respectively. WMD acronyms are shown. Latitudes are given on the left side and longitudes at the top. Lake Okeechobee can be seen in the southeast part of the state.

were provided by three of the WMDs (SF, SJR, and SWF) and the remaining data were obtained from the University of Florida, Institute of Food and Agricultural Sciences, Florida Automated Weather Network website (http://www.fawn.ifas.ufl.edu), and the U.S. Geological Survey (USGS). Datasets from 57 stations were used, divided into three groups, referred to in this work as "Group 1," "Group 2," and "Group 3." Groups 2 and 3 data were used for calibration purposes while Group 1 data were used for GDM performance assessment. The locations and details of each of the stations in these groups are shown in Figure 1 and Table 1. For performance assessment (Group 1), we used nine stations – 2 from each WMD region (except NWF, only one quality station available) so that each region would be represented; these stations had good data quality over the longest available data records. For the other two groups (Groups 2 and 3), used for the calibration coefficient derivations, high-quality data were needed, which meant using many different stations over the 10-year period as a means of having enough quality information.

Each weather station network used the LI-COR 200 pyranometer produced by LI-COR, Inc. (Lincoln, Nebraska), with recalibration performed every 1 to 2 years. This silicon cell device has a quoted accuracy of 5%. Pyranometer site locations varied from open fields to water bodies (lakes and bays), but the latter were avoided whenever possible to minimize issues such as salt deposit contamination of the sensors. Temporal resolution of the pyranometer data ranged from 15 min to 1 h averages (see Table 1) and daily integrated insolation values were calculated using the midpoint integration method.

A practical issue to be considered for the calibration activity was choosing good quality data. Most of the data were provided with quality assurance and quality control (QA/QC) flags, but these flags were not infallible. For example, some stations consistently underestimate clear-sky insolation in comparison with empirical estimates. As a result, an additional method for screening the data, developed by the American Society of Civil Engineers, was employed (see Allen *et al.*, 2005, Appendix D). This method involved comparing daily integrated insolation data with estimated clear-sky radiation, R_{so} (MJ m^{-2}/day), estimated as a function of station elevation (z) and extraterrestrial radiation (R_a: short-wave solar radiation in the absence of an atmosphere) over a 24-h period by

$$R_{so} = (0.75 + 2 \times 10^{-5} z) R_a, \tag{1}$$

where R_a is a function of day of year, solar constant, solar declination, and latitude, given by

$$R_a = \frac{24}{\pi} G_{sc} d_r [\omega_s \sin(\varphi)\sin(\delta) + \cos(\varphi)\cos(\delta)\sin(\omega_s)] \tag{2}$$

Here, G_{sc} is the solar constant (4.92 MJ m^{-2}/h), d_r is the inverse relative distance factor (squared) for the earth-sun (unitless), ω_s is the sunset hour angle (radians), φ is latitude (radians), and δ is the solar declination (radians) (see Duffie and Beckman, 1980; Allen, 1996; Allen *et al.*, 2005, Appendix D for further details).

The assumption is that measured daily insolation should be close to estimated clear-sky values on at least some days during the year – those days being considered as cloud-free. When examining annual bell curve plots of this comparison, it was possible to identify when a station had significant data quality issues not indicated by QA/QC flags; specifically, under complete sunshine, quality pyranometer measurements should be near the R_{so} values. For pyranometer data not provided with any QA/QC information, the above method was employed as an initial filter, following that, data greater than 105% of the estimated clear-sky value were removed (Allen *et al.*, 2005). These methods eliminated stations, or periods of the data record, that appeared erroneous.

Satellite-Pyranometer Data Differences

There are inherent differences between satellite-estimated and pyranometer-measured solar insolation data. At the pixel level, satellite data provide a snapshot at a given time, with each pixel in the snapshot

TABLE 1. Pyranometer Dataset Information.[1]

Station No.	Group	Network	Station	County	Latitude (°)	Longitude (°)	Date	Days	Resolution (min)
1	1	FAWN	Alachua	Alachua	29.80	82.41	16Oct99	1,191	15
2	1	FAWN	Bronson	Levy	29.40	82.59	26Sep02	794	15
3	1	FAWN	Quincy	Gadsden	30.54	84.60	13Sep02	460	15
4	1	SF WMD	ENR308	Palm Beach	26.62	80.44	1Jun95	2,187	30[3]
5	1	SF WMD	S65CW	Okeechobee	27.40	81.11	1Sep99	1,833	30[3]
6	1	SJR WMD	Orange Lake	Alachua	29.48	82.13	14Feb97	689	30[3]
7	1	SJR WMD	Tucker	Brevard	27.83	80.81	1Sep96	838	30[3]
8	1	SWF WMD	Floral City	Citrus	28.76	82.28	1Jun95	3,209	60
9	1	SWF WMD	Inglis	Levy	29.03	82.62	1Jun95	3,196	60
10	2	SF WMD	BCSI	Hendry	26.32	81.07	N/A[2]	2	30[3]
11	2	SF WMD	CFSW	Hendry	26.74	80.90	N/A[2]	2	30[3]
12	2	SF WMD	ENR105	Palm Beach	26.66	80.41	N/A[2]	3	30[3]
13	2	SF WMD	JDWX	Martin	27.03	80.17	N/A[2]	1	30[3]
14	2	SF WMD	L001	Okeechobee	27.14	80.79	N/A[2]	6	30[3]
15	2	SF WMD	L005	Glades	26.96	80.97	N/A[2]	1	30[3]
16	2	SF WMD	S61W	Osceola	28.14	81.35	N/A[2]	2	30[3]
17	2	SF WMD	S65DWX	Okeechobee	27.31	81.02	N/A[2]	7	30[3]
18	2	SF WMD	S75WX	Glades	27.19	81.13	N/A[2]	1	30[3]
19	2	SF WMD	S78W	Glades	26.79	81.30	N/A[2]	1	30[3]
20	2	SF WMD	S140W	Broward	26.17	80.83	N/A[2]	3	30[3]
21	2	SF WMD	SGGEWX	Collier	26.15	81.58	N/A[2]	1	30[3]
22	2	SF WMD	SILVER	Collier	26.30	81.44	N/A[2]	1	30[3]
23	2	SF WMD	WRWX	Polk	28.05	81.40	N/A[2]	5	30[3]
24	2	SJR WMD	Bull Creek	Osceola	28.08	80.96	N/A[2]	1	30
25	2	SJR WMD	Elkton	St. Johns	29.78	81.44	N/A[2]	4	60
26	2	SJR WMD	Ft. Drum	Indian River	27.59	80.69	N/A[2]	3	30[3]
27	2	SJR WMD	Hell Cat Bay	Putnam	29.60	81.53	N/A[2]	4	60
28	2	SJR WMD	Lake Jessup	Seminole	28.75	81.21	N/A[2]	1	30[3]
29	2	SJR WMD	Lindsey Citrus	Indian River	27.58	80.60	N/A[2]	2	30
30	2	SJR WMD	Mulberry Marsh	Brevard	27.91	80.78	N/A[2]	1	30
31	2	SJR WMD	Ocklawaha Prairie	Marion	29.10	81.91	N/A[2]	2	30
32	2	SJR WMD	Orange Creek	Alachua	29.46	82.07	N/A[2]	3	30
33	2	SWF WMD	Avon Park	Highlands	27.60	81.48	N/A[2]	1	60
34	2	SWF WMD	Bowling Green	Hardee	27.64	81.84	N/A[2]	4	60
35	2	SWF WMD	Headquarters	Hernando	28.47	82.44	N/A[2]	8	60
36	2	SWF WMD	Lake Como	Pasco	28.18	82.47	N/A[2]	7	60
37	2	SWF WMD	Peace River	Desoto	27.09	82.00	N/A[2]	1	60
38	2	SWF WMD	Wildwood	Sumter	28.86	82.03	N/A[2]	5	60
39	3	FAWN	Apoka	Orange	28.64	81.55	1Jan98	2,424	15
40	3	FAWN	Avalon	Orange	28.47	81.65	13Mar99	1,993	15
41	3	FAWN	Balm	Hillsborough	27.76	82.22	17Dec03	361	15
42	3	FAWN	Brooksville	Hernando	28.63	82.28	25Apr00	1,658	15
43	3	FAWN	Dover	Hillsborough	28.02	82.23	15Aug98	2,242	15
44	3	FAWN	Ft. Lauderdale	Broward	26.09	80.24	25Jan01	1,387	15
45	3	FAWN	Ft. Pierce	St. Lucie	27.43	80.40	10Jul98	2,275	15
46	3	FAWN	Hastings	St. Johns	29.69	81.44	5Aug99	1,919	15
47	3	FAWN	Homestead	Dade	25.51	80.50	1Jan98	2,463	15
48	3	FAWN	Immokalee	Collier	26.46	81.44	1Jan98	2,442	15
49	3	FAWN	Lake Alfred	Polk	28.10	81.71	1Jan98	2,456	15
50	3	FAWN	Live Oak	Suwanee	30.30	82.90	18Sep02	804	15
51	3	FAWN	Marianna	Jackson	30.85	85.17	12Sep02	809	15
52	3	FAWN	Ocklawaha	Marion	29.02	81.97	23Mar99	2,041	15
53	3	FAWN	Okahumpka	Lake	28.68	81.89	2Feb99	1,976	15
54	3	FAWN	Ona	Hardee	27.40	81.94	11Mar98	2,395	15
55	3	FAWN	Pierson	Volusia	29.22	81.45	24May99	1,975	15
56	3	FAWN	Putnam Hill	Putnam	29.70	81.98	25Jan01	1,323	15
57	3	USGS	Lake Starr	Polk	27.96	81.59	21Jul96	2,973	60

Notes: FAWN, Florida Automated Weather Network; SF, South Florida; SJR, St. Johns River; SWF, Southwest Florida; USGS, U.S. Geological Survey; WMD, Water Management Districts.

[1]Pyranometer station: dataset group number, network agency, name, location, begin date of data record used, number of data days used, and temporal resolution (also data-averaging period unless otherwise noted).

[2]Dates are individual days, refer to Table 3.

[3]Fifteen-minute averaging period, every second data record used.

having a single value, that being the spatial average over the horizontal surface pixel area. Pyranometer data, on the other hand, are generally time-averaged. So in the case of the satellite instrument, insolation data are spatially smoothed, whereas pyranometer data are temporally smoothed. These differences do not cause significant data disparities under cloud-free conditions (when solar insolation is homogeneous over a given region) but become an increasing issue as cloud cover variability and data temporal resolution increase. Both the use of high-resolution satellite data and temporal averaging blurs these disparities, the latter being demonstrated via the differences in hourly *vs*. daily integrated insolation errors quoted in the sections titled Introduction and The Solar Insolation Model.

MODEL CALIBRATION

As discussed in the section titled The Solar Insolation Model, the GDM performs well over a variety of land-surface and climatic conditions, as well as spatial and temporal resolutions. In the current study, daily integrated GOES-estimated insolation data were further fine-tuned through a cumulative three-step process via comparison with ground-based pyranometer data (hereafter referred to as "calibration"). First, the initial insolation data estimated via the GDM (referred to as "DAILY_A") were compared with pyranometer observations on a series of clear (non-cloudy) reference days resulting in a set of calibration coefficients, the application of which produced the "DAILY_B" dataset. Second, a "cloudiness" bias correction was derived from, and applied to, the DAILY_B data, resulting in the "DAILY_C" dataset. Lastly, a monthly correction factor was calculated from, and applied to the DAILY_C data, yielding the final dataset "DAILY_D." These steps are discussed in detail in the sections below. For each calibration step, the GOES-estimated and pyranometer insolation data were matched spatially by choosing the satellite data pixel that each pyranometer station was located "within."

For GDM performance assessment, each of the above datasets are compared with pyranometer data from the "Group 1" dataset, consisting of nine calibration-independent surface stations located across Florida as detailed in Figure 1 and Table 1. The results, showing the calibration progression, are shown for the entire data period and each of the nine station locations in Figure 2. Statistics used for this comparison (quoted on each plot) are the RMSE (also expressed as a percentage of the mean pyranometer observed value), the mean bias error (MBE), and the coefficient of determination (R^2). Table 2 and Figure 3a present station-averaged statistics and seasonal station-averaged model MBE, respectively. Note that the number of stations in the averaged statistics (Figure 3b) varies from 2 to 7, subject to the data record length of each station and the necessity for quality data for comparison. Similar comparisons using the half-hourly resolution insolation could not be made since calibration was only performed for the daily insolation product.

Initial Results

Station-averaged calibration statistics from the initial dataset (DAILY_A: Figures 2 and 3 and Table 2) are as follows: coefficient of determination 0.90, MBE −0.7 MJ m^{-2}/day, and RMSE 2.2 MJ m^{-2}/day (13% of the mean observed value). These statistics indicates performance slightly poorer than previous studies using the GDM, which generally had RMSE values of about 10% of the mean observed value for daily integrated insolation comparisons (see the section titled The Solar Insolation Model). Figure 3a shows a predominantly negative bias in model-estimated daily insolation values, gradually increasing to a slight positive bias beyond mid-2003, with about a 4 MJ m^{-2}/day difference from the beginning to the end of the 10-year historical data period. A seasonal bias oscillation on the order of ±0.5 MJ m^{-2}/day is also present, with MBE values tending to be more positive during the summer and autumn seasons. This trend is clearer in the latter years of the data period (2001 onward), with increasing numbers of stations in the average (see Figure 3b). Due to the larger number of stations, this seasonal trend is more evident when comparing with the pyranometer data of the "Group 3" dataset (see Section Pyranometer Data) – the station average MBE, which is also plotted in Figure 3a (Group 3 DAILY_B). These observations are discussed further in the section titled Discussion of Calibration Issues.

The scatter plots of Figure 2 reveal an overestimation and underestimation of insolation by the GDM under clear and cloudy conditions, respectively – with the latter being most prevalent. The occasional data point where pyranometer data were significantly underestimating insolation is also observed, which may be due to the so-called "bird effect" – when birds use the pyranometer as a perch and shade the sensor (personal communication with USGS staff). The approach we use to fine-tune and correct the data for some of these observations are described in the following sections.

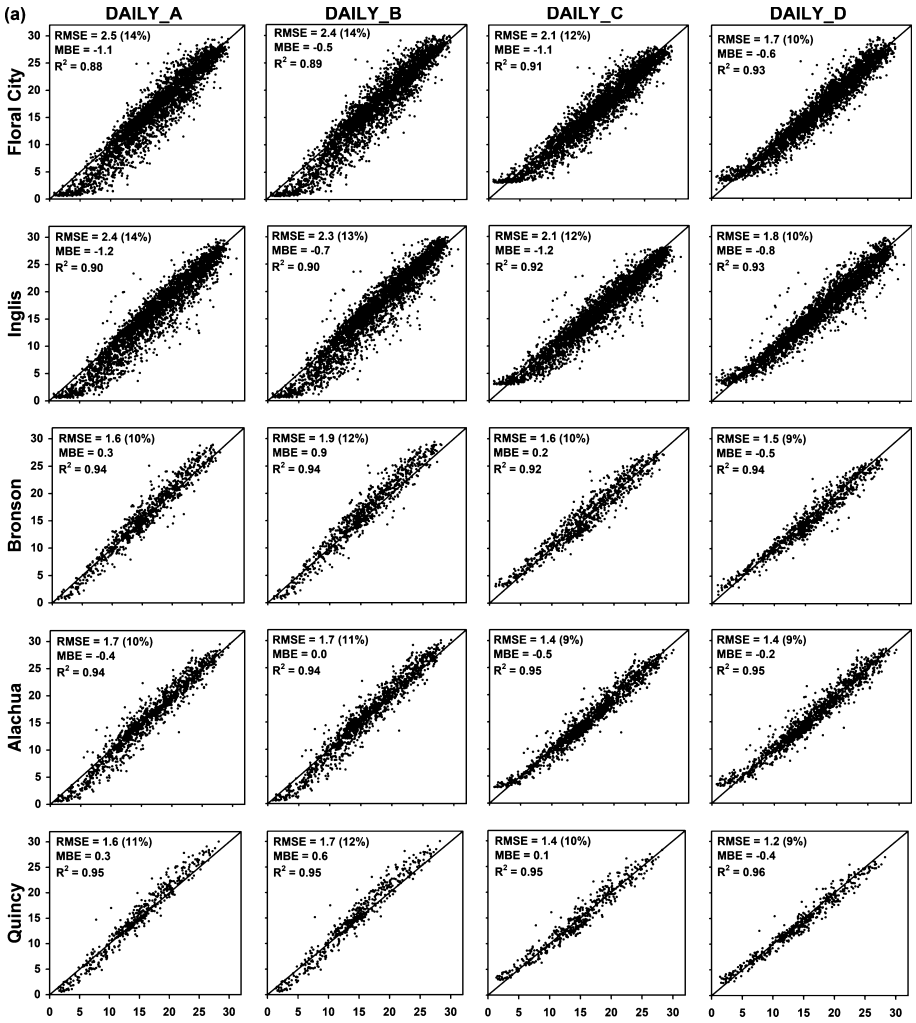

FIGURE 2. Comparison of Satellite-Estimated (ordinate) and Pyranometer-Measured (abscissa) Daily Integrated Insolation [MJ m^{-2}/day] for the Nine Model Calibration Locations. Station names are given along the left-side, and comparison satellite-estimated dataset names are indicated at the top. RMSE values [MJ m^{-2}/day] and as a percentage of the mean observed value (in parentheses), MBE [MJ m^{-2}/day], and coefficient of determination for each station and dataset are quoted for each comparison.

Clear-Day Comparison

On a clear day, disparities between satellite-estimated and pyranometer-measured insolation should be minimized, as without clouds solar insolation received at the surface will locally be spatially homogeneous, providing reference conditions for the comparison of the two datasets. This "clear-day comparison" was made on a day as free of cloud as possible over Florida every 6 months – 1 day in each summer and winter season (or as close as possible). Completely clear days over the entire state of Florida are rare, and therefore many times the comparison was limited to available cloud-free regions. Additionally, due to factors such as site decommissioning, periods of missing data, instrument issues, and variations in data quality, it was not possible to use a single set of pyranometer stations for the entire 10-year study period, but continuity was maintained as much as possible.

For each clear day, the half-hourly satellite insolation product was compared with "Group 2" pyranometer data for up to three stations within each of the SF, SJR, and SWF WMD regions (no data were available for NWF or SR for this analysis). Pyranometer data time-stamps were adjusted to the middle of their data-averaging period and GOES data times were used unmodified. For each WMD region, the satellite and corresponding pyranometer datasets were averaged (across the selected stations), resulting in two datasets (GOES satellite and pyranometer). These two averaged datasets were then plotted, and the satellite data calibration coefficient for each WMD was determined by multiplying the averaged satellite

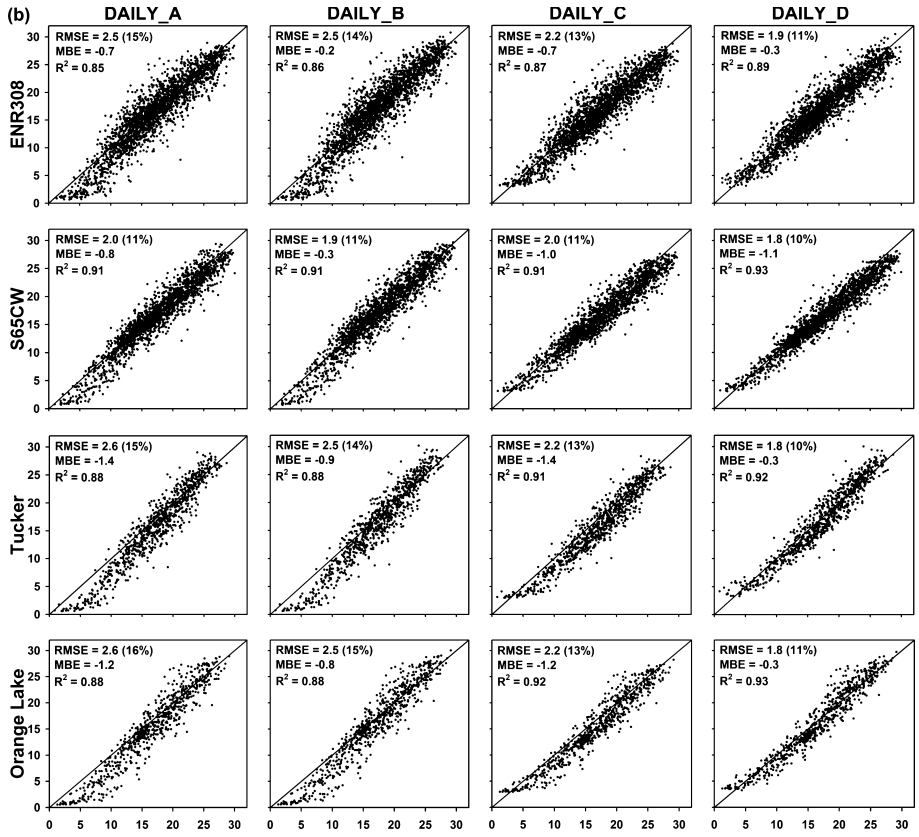

FIGURE 2. (Continued)

TABLE 2. Calibration and Comparison Station-Averaged Statistics for Data Period.[1]

	DAILY_A	DAILY_B	DAILY_C	DAILY_D
RMSE MJ m^{-2}/day (%)	2.2 (13)	2.2 (13)	1.9 (11)	1.7 (10)
MBE MJ m^{-2}/day	−0.7	−0.2	−0.8	−0.5
R^2	0.90	0.91	0.92	0.93

Notes: MBE, mean bias error; RMSE, root mean square error.
[1]RMSE as percentage of mean observed value given in parentheses.

data by a factor necessary for its diurnal insolation curve to align with the averaged pyranometer data curve as closely as possible. This factor was manually determined as a means of correcting for the satellite-pyranometer differences. Subsequently, the average of all available WMD correction factors were taken to obtain a calibration coefficient for that particular day for application over the entire state of Florida. This process was carried out for the entire observation period, resulting in a set of 20 approximately biannual calibration coefficients spanning the 10-year data record, as shown in Table 3. The individual coefficients, obtained only on days when pyranometer data were available, were then interpolated in time to obtain a calibration coefficient set that could be applied to each day across the data record.

As a check for potential issues, calibration factors using the above method were obtained for 3 consecutive clear days (March 6-8, 2001, results not shown in Table 3). During these days weather conditions remained consistent over Florida, implying that if the application of the GDM in this study was successful, the same should be the case of the three calibration factors. This was the case: the calibration coefficient of each day had a value of 1.09.

For the model calibration, these coefficients were applied to the initial (DAILY_A) data, yielding the DAILY_B dataset. The results of this calibration are shown in Figures 2 and 3 and Table 2. The station-averaged RMSE remained the same as that of the initial dataset, the coefficient of determination increased to 0.91, and the average MBE decreased in magnitude from −0.7 to −0.2 MJ m^{-2}/day (Table 2). Figure 3 reveals that although the MBE has been reduced on average, the temporal trend of MBE (positive shift with time) is still present, with a similar range (from dataset beginning to end) as the

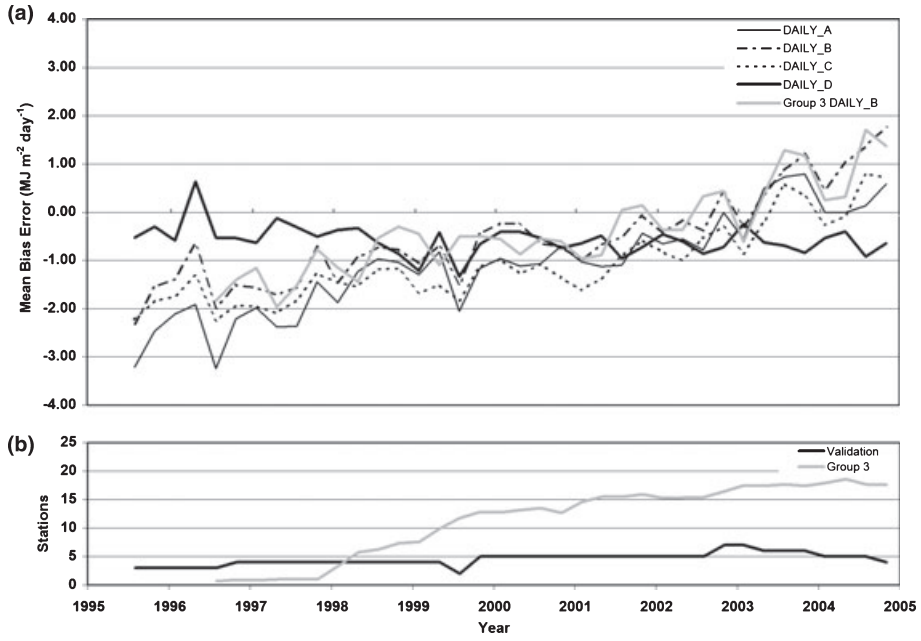

FIGURE 3. (a) Season and Station-Averaged Daily Integrated Solar Insolation MBE and (b) Number of Stations in the Average at Any Given Time. "Group 3" dataset is included in both (a and b) for comparison as discussed in Clear-Day Comparison section. Season months are December to February (winter), March to May (spring), etc.

initial dataset. The seasonal MBE oscillation is also still present, as is the cloudiness-related bias (see Figure 2). The following sections address these remaining issues.

Cloudiness Bias Correction

In an effort to correct for the cloudiness-related bias in model data, a "cloudiness" bias correction was developed using the DAILY_B satellite-estimated insolation dataset (the product of the clear-day calibration). These data were compared with pyranometer data from the "Group 3" dataset with model bias values calculated for each individual station and day combined (but not averaged), and plotted *vs.* "cloudiness index" (Figure 4). The cloudiness index is defined here as the ratio of the Daily_B satellite-estimated insolation and estimated daily clear-sky solar insolation, R_{so}.

Examination of Figure 4 reveals a model bias [MJ m^{-2}/day] approximated as linearly related to cloudiness by

$$\text{Cloudiness\_bias} = 4.44[\text{Cloudiness\_index}] - 2.55 \qquad (3)$$

The cloudiness bias given by Equation (3) was calculated for each comparison station and day and subtracted from the DAILY_B data, resulting in the DAILY_C dataset. Examination of this dataset revealed that the bias related to cloudiness was then found to be negligible, reflected by an increase in the

TABLE 3. Calibration Coefficients Determined by Clear-Day Comparison of Satellite-Estimated and Pyranometer-Measured Solar Insolation.[1]

Date	SF	SJR	SWF	Average
14Jun95	1.05 (11, 20)	N/A[2]	N/A[2]	1.05
22Nov95	1.12 (20)	1.14 (25, 27)	1.12 (35, 36)	1.13
28Jul96	1.03 (19, 20)	N/A[2]	N/A[2]	1.03
14Dec96	1.11 (12)	1.10 (25, 27)	1.08 (36)	1.10
4May97	N/A[2]	1.06 (25, 27)	1.06 (38)	1.06
17Dec97	1.08 (12)	1.14 (28)	1.10 (38)	1.11
13May98	1.03 (12, 13)	1.03 (26)	1.04 (38)	1.03
16Dec98	N/A[2]	1.06 (25, 27)	1.08 (36)	1.07
13Apr99	1.06 (11, 14, 15)	1.07 (26)	1.04 (35, 36)	1.06
24Dec99	1.10 (16)	1.12 (26)	1.07 (35, 36)	1.10
20May00	1.04 (10, 14)	N/A[2]	1.04 (35, 36)	1.04
30Nov00	1.06 (14, 17)	N/A[2]	1.05 (36)	1.05
17May01	1.05 (10, 17)	N/A[2]	1.01 (33, 34)	1.03
21Dec01	1.08 (14, 17, 22)	N/A[2]	1.07 (35)	1.08
3May02	1.06 (16, 17, 23)	N/A[2]	1.01 (34, 37)	1.04
29Dec02	1.12 (14, 17, 23)	N/A[2]	1.07 (35)	1.10
13Apr03	1.03 (21, 23)	N/A[2]	1.01 (34, 35)	1.02
20Dec03	1.11 (17, 23)	1.10 (24, 30, 32)	1.07 (34, 35)	1.09
28Apr04	1.08 (17)	1.07 (29, 31, 32)	1.04 (38)	1.06
12Dec04	1.12 (14, 18, 23)	1.12 (29, 31, 32)	1.09 (38)	1.11

Notes: SF, South Florida; SJR, St. Johns River; SWF, Southwest Florida; WMD, Water Management Districts.

[1]Clear-day date, average coefficient for each WMD region, and average of all regions. Numbers in parentheses indicate stations used in the analysis (see Table 1).

[2]Comparison not possible due to lack of data or cloud cover.

coefficient of determination to 0.92 and decrease in the average RMSE from 2.2 to 1.9 MJ m^{-2}/day (Table 2). This improvement is also evident in Figure 2: although the low end of the model data has been somewhat "raised," this affects only a small percentage of the data, and for the ultimate purpose of this dataset (the estimation of ET), this is not considered to be a significant issue since the component of ET due to solar insolation will be small on these cloudy (and/or rainy) days.

Table 2 reveals that with this bias correction the station and time-averaged MBE became more negative, increasing in magnitude from −0.2 to −0.8 MJ m^{-2}/day. Figure 3 indicates that the issues of predominantly negative model data bias, positive shift of MBE with time and seasonal MBE oscillation still remain. These issues were addressed with the next calibration step.

Monthly Bias Correction and Final Data Product

The final calibration step was the development of a monthly bias correction. DAILY_C model and "Group 3" pyranometer data were averaged over all calibration stations for each data month. The latter were then subtracted from the former, resulting in a set of monthly bias correction coefficients spanning the data period. [Note: due to data availability and time constraints, June 1996 through June 1997 coefficients were used for the June 1995 through June 1996 period. This was deemed acceptable as the most important bias features (e.g., the seasonal oscillation) were captured by this surrogate set of coefficients.] These bias corrections were then subtracted from the DAILY_C data, giving us the final dataset, "DAILY_D." The results of this adjustment are presented in Figures 2 and 3 and Table 2.

The result of this procedure is that the station-averaged statistics all improved. The average RMSE and MBE values decreased in magnitude to 1.7 (10% of the mean observed value) and −0.5 MJ m^{-2}/day, respectively, and the coefficient of determination increased to 0.93. In comparison with the initial dataset (DAILY_A), the RMSE and MBE decreased in magnitude by 0.5 and 0.2 MJ m^{-2}/day, respectively, and the coefficient of determination rose by 0.03. Although the average MBE is still negative and of greater magnitude than the result of the DAILY_B calibration, Figure 3 shows that the effect of this calibration step was the removal of both the seasonal oscillation and the positive shift of MBE with time, with the station average ranging between about −1 and 0 MJ m^{-2}/day across the data record period.

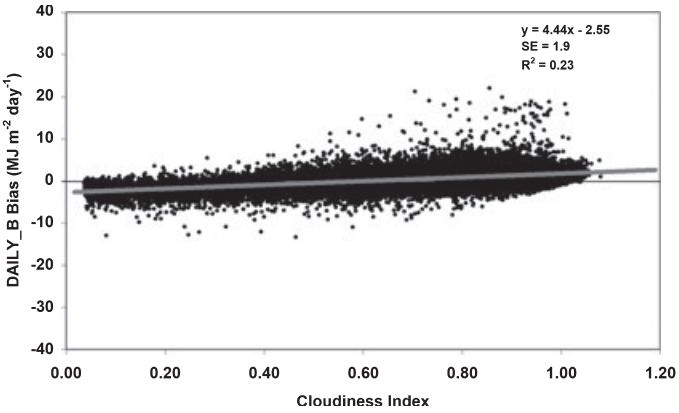

FIGURE 4. Model Bias *vs*. Cloudiness Index for DAILY_B Dataset. Standard error [MJ m^{-2}/day] and coefficient of determination are given.

DISCUSSION OF CALIBRATION ISSUES

Change in Model Bias With Time

Although the gains made by this calibration work may be seen as minimal compared with the effort invested, it may have been worthwhile just to have discovered and removed the GDMs positive shift of MBE with time as this temporal bias likely would introduce a spurious trend into computed ET (see section titled Insolation Error Propagation into Reference and Potential ET Estimation). The cause of this trend is unclear. It is not a function of the number of calibration stations in the statistical average (which also generally increased with time, see Figure 3b) as it is also evident in single station MBE analyses. When comparing the initial dataset (DAILY_A) station-averaged MBE with that of the Otkin *et al.* (2005) GOES East satellite analysis over the 15-month period of their work (December 2002 to February 2004), essentially the same result is found (0.3 and 0.4 MJ m^{-2}/day, respectively), with the GDM tending to slightly overestimate daily insolation values in both cases. Although the short length of this comparison period and the averaging of statistics are not sufficient to make any qualified conclusions, the indication, given the range of comparison site characteristics and climates of the two studies, is that something independent of these is causing this effect. It is possible that issues pertaining to the GOES satellite data may be responsible, for example sensor degradation caused by dust accumulating on the visible sensors lens itself. It is believed that in both studies, this one and that of Otkin *et al.* (2005), the expected effects were to see signs of the GOES-8 visible sensor's degradation with the aging of the satellite, but this was not clearly apparent. Addition-

ally, on April 1, 2003, the GOES-12 satellite took over operations from the GOES-8 satellite. With the fresh sensors on board the new spacecraft, we expected to see a sudden change in the model data bias, but again this was not evident in these data. It is believed that in both cases, the expected effects are not clearly seen because they are masked by the inherent limitations of the GDM and this particular application of it. Although this issue of satellite sensor degradation has not been directly addressed, the effects of it have been indirectly corrected for through the calibration process of this work.

Seasonal Bias Oscillation

With regard to the seasonal oscillation observed in the model data MBE, both Pinker *et al.* (2003) and Otkin *et al.* (2005) observed such an oscillation over the 1-year to 2-year periods of their analyses, with the MBE generally being more positive in the summer months. Comparing the initial dataset with the GOES East satellite analysis of Otkin *et al.* (2005) for the time period of their work, but now on a seasonal basis, similar station-averaged MBE values were found. As for the increase in model bias trend with time, the reason for this seasonal trend is also unclear; it is not due to cloudier conditions during the Florida summer, as (discussed in the section the Cloudiness Bias Correction) the GDM tends to underestimate rather than overestimate insolation under cloudy conditions. It may simply be due to inherent limitations of the GDM algorithm, for example seasonal sun-angle effects that are not accounted for. Fortunately, and regardless of the cause, this bias oscillation was estimated to be small, even in the initial dataset.

Comparison With Previous Studies

The RMSE of 10% of the mean observed value for the final dataset is comparable with the (un-calibrated) results of previous studies. We believe this might be because of the complex and prevalent cloud conditions of Florida relative to previous study areas, leading to a particularly challenging application of the model. Previous studies have found that as cloudiness increased GDM performance decreased. Gu *et al.* (1999) found coefficient of determination values of 0.96, 0.77, and 0.59 for half-hourly observations during clear, partly cloudy, and cloudy conditions, respectively, over forested regions of central Canada. Otkin *et al.* (2005) found similar results, with lower coefficients of determination and higher RMSE values in the complex cumulus cloud environments of summer months. The study of Jacobs *et al.* (2002) over northern-central Florida reported a similar conclusion in comparison with studies over less convective-cloud-prone locations and seasons. Results from the GOES component of the GEWEX SRB product (Meng *et al.*, 2003) show that RMSEs are near 32 Wm^{-2} for their 0.5° shortwave radiation product.

Further Dataset Applications

The data-mining possibilities for such a dataset are vast. As an example, Figure 5 shows the 9-year (1996-2004) mean daily solar insolation for the state of Florida for January 1 and the month of January. Similarly, Figure 6 shows the 10-year (1995-2004) mean for July 1 and the month of July. (The 10-year average is not available for January because the dataset begins in June 1995.) These images reveal spatial biases in solar insolation including the generally cloudier conditions over land than sea; chronic clear-sky conditions over Lake Okeechobee; relatively clear-sky conditions in SWF compared to the cloudier southeast coast in January; and hints of an urban heat island-induced clear-sky bias in the cities of Orlando and Jacksonville.

Such data could also serve for applications such as detailed radiation monitoring to detect climate change (in the radiation component of climate), and in the resulting impacts on ET. Furthermore, the method described in this work could be applied to any region in the world for which the appropriate satellite and pyranometer data are available. It should be noted that a full network of pyranometers (as used in this study) is desirable for product calibration, yet because this is cost-prohibitive, less than 20 instruments distributed across an area such as the state of Florida would suffice.

Insolation Error Propagation into Reference and Potential ET Estimation

Given that the insolation data, developed here as a long-term climatology, are valuable for determining ET (reference and potential), it is useful to discuss how errors in insolation propagate through to errors in ET. Analysis of the procedures that relate solar insolation to potential and reference ET suggests that potential ET is perhaps more influenced by errors in insolation because the computations cannot be offset by an aerodynamic component, which is present in the reference ET equations (Dave Sumner-USGS and Jennifer Jacobs-University

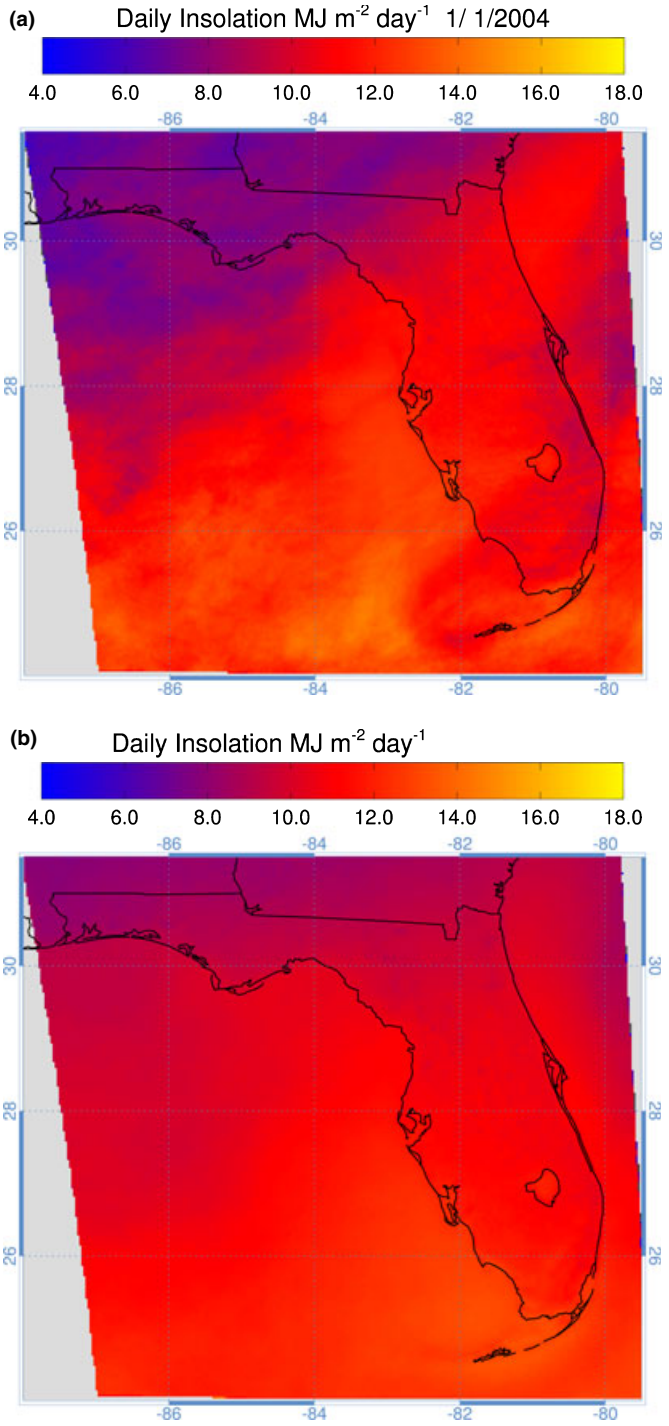

FIGURE 5. The 9-Year (1996-2004) Mean Daily Solar Insolation for January 1 (a) and the Month of January (b).

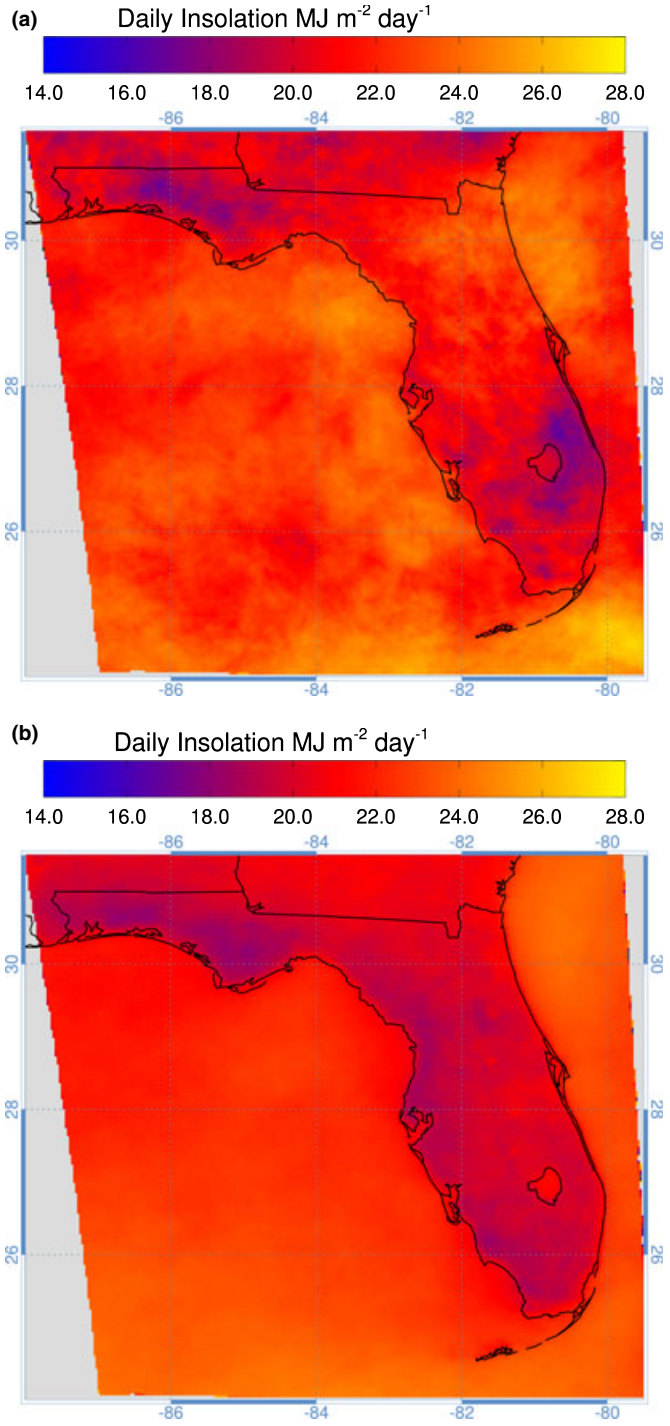

FIGURE 6. The 10-Year (1995-2004) Mean Daily Solar Insolation for July 1 (a) and the Month of July (b).

of New Hampshire, personal communications). For example, it is understood that via the Priestley-Taylor approach (Priestley and Taylor, 1972) as used by the USGS, potential ET is directly proportional to net radiation, and specifically to the shortwave component. Also, solar insolation enters into the longwave calculation of potential ET through atmospheric emissivity, which is especially important during clear skies, as they produce more negative net daily longwave radiation. In this light, we estimate that a 10% error in insolation causes a 5-6% error in ET is somewhat higher for potential ET.

This error will be higher in summer, with more longwave radiation at this time of year and lower surface resistances (aerodynamic and soil), than in winter (USGS, personal communications).

SUMMARY AND CONCLUSION

GOES satellite estimates of incoming solar radiation (insolation) for the state of Florida have been made using the model of Gautier *et al.* (1980) (the "GDM") for the period June 1995 to December 2004. The dataset has been produced with 2 km spatial, and half-hour and daily temporal resolution. In addition, a 2-week running minimum surface albedo product was generated, also at 2 km resolution. Through comparison with ground-based pyranometer data, a series of cumulative calibration steps were developed to de-bias and fine-tune the daily integrated insolation product.

It was found that the initial (uncalibrated) GDM product (DAILY_A) performed well, but slightly poorer than previous studies, with a calibration station-averaged value of the coefficient of determination of 0.90, MBE of -0.7 MJ m^{-2}/day, and RMSE of 2.2 MJ m^{-2}/day (13% of the mean observed value). The model data had a predominantly negative bias that became increasingly positive with time over the data record period. A seasonal bias oscillation was also discovered, with MBE values tending to be more positive in the summer and autumn seasons. Additionally, the model was found to overestimate and underestimate solar insolation under clear and cloudy conditions, respectively, with the latter being most evident.

Following the three calibration steps, the final product (DAILY_D) showed improvements in comparison with the initial dataset, with the station-averaged coefficient of determination increasing to 0.93, and MBE and RMSE values decreasing in magnitude to -0.5 and 1.7 MJ m^{-2}/day, respectively. Perhaps, the most significant effect of this calibration effort was to remove both the positive shift of model bias with time and the seasonal bias oscillation. The final dataset RMSE (10% of the mean observed value) is comparable with the (un-calibrated) results of previous studies. It is believed this may be due to the cloudy conditions of Florida relative to previous study areas, leading to a particularly challenging application of the model.

Solar insolation is the largest determinant for temporal variation in ET in *wet* regions, like those often found across the state of Florida (when soil water is never limiting and the advection of heat is absent), and hence is a critical variable in water management efforts. The most desirable ET datasets for these purposes are spatially continuous, rather than those with point values derived from traditional field station networks. Thus, mapping of ET over large regions is greatly facilitated by satellite-derived estimates of the spatial distribution of solar insolation. This study's final (potential and reference) ET product will be used in such an effort, by the five Florida WMDs. Work is underway to continue data production (2005 to present) and provide ongoing annual dataset updates.

Additional applications for this dataset are numerous, and include via the reference ET field, solar energy estimation, irrigation scheduling, water allocation management, and crop-type planting decisions. Solar insolation to formulate potential ET can be used as input into surface and groundwater hydrological models (such as the USGS MODFLOW groundwater flow model, MikeShe and HSPF subsurface and surface water models), as well as for wildlife and wild-land monitoring. The solar insolation data themselves may be used as boundary conditions in ecosystem modeling and oceanic modeling. Furthermore, the GDM method could be applied to any region in the world for which the appropriate satellite data (and pyranometer data for calibration) are available, thereby providing such observations for remote, inaccessible, or hazardous regions, large water bodies, or for countries that do not have the means to install a ground-based observation network.

ACKNOWLEDGMENTS

We would like to thank the following people for their contributions, cooperation, and patience that made this work possible: George Robinson of St. Johns River WMD, Michael Hancock of Southwest Florida WMD, and Jennifer Jacobs of the University of New Hampshire. We also acknowledge funding support for this project from the State of Florida WMD: St. Johns River, South Florida, Southwest Florida, Suwannee River, and Northwest Florida. This work was made possible by U.S. Geological Survey Research Grant 05ERAG0027.

LITERATURE CITED

Allen, R.G., 1996. Assessing Integrity of Weather Data for Use in Reference Evapotranspiration Estimation. Journal of Irrigation and Drainage Engineering, ASCE 122:97-106.

Allen, R.G., I.A. Walter, R.L. Elliott, T.A. Howell, D. Itenfisu, M.E. Jensen, and R.L. Snyder, 2005. The ASCE Standardized Reference Evapotranspiration Equation. American Society of Civil Engineers, Reston, Virginia.

Anderson, M.C., W.L. Bland, J.M. Norman, and G.R. Diak, 2001. Canopy Wetness and Humidity Prediction Using Satellite and Synoptic-Scale Meteorological Observations. Plant Disease 85:1018-1026.

Anderson, M.C., W.P. Kustas, and J.M. Norman, 2003. Upscaling and Downscaling – A Regional View of the Soil-Plant-Atmosphere Continuum. Agronomic Journal 95:1408-1432.

Anderson, M.C., J.M. Norman, J.R. Mecikalski, R.D. Torn, W.P. Kustas, and J.B. Basara, 2004. A Multiscale Remote Sensing Model for Disaggregating Regional Fluxes to Micrometeorological Scales. Journal of Hydrometeorology 5:343-363.

Cosgrove, Brian A., Dag Lohmann, Kenneth E. Mitchell, Paul R. Houser, Eric F. Wood, John Schaake, Alan Robock, Curtis Marshall, Justin Sheffield, Lifeng Luo, Qingyun Duan, Rachel T. Pinker, J. Dan Tarpley, R. Wayne Higgins, and Jesse Meng, 2003a. Realtime and Retrospective Forcing in the North American Land Data Assimilation Systems (NLDAS) Project. Journal of Geophysical Research 108(D22):8842, doi: 10.1029/2002JD003118.

Cosgrove, Brian A., Dag Lohmann, Kenneth E. Mitchell, Paul R. Houser, Eric F. Wood, John C. Schaake, Alan Robock, Justin Sheffield, Qingyun Duan, Lifeng Luo, R. Wayne Higgins, Rachel T. Pinker, and J. Dan Tarpley, 2003b. Land Surface Model Spin-up Behavior in the North American Land Data Assimilation System (NLDAS). Journal of Geophysical Research 108(D22): 8845, doi: 10.1029/2002JD003119.

Darnell, W.L., W.F. Staylor, S.K. Gupta, and F.M. Denn, 1988. Estimation of Surface Insolation Using Sun-Synchronous Satellite Data. Journal of Climate 1:820-835.

Dedieu, G., P.Y. Deschamps, and Y.H. Kerr, 1987. Satellite Estimates of Solar Irradiance at the Surface of the Earth and of Surface Albedo Using a Physical Model Applied to Meteosat Data. Journal of Climate and Applied Meteorology 26:79-87.

Diak, G.R., M.C. Anderson, W.L. Bland, J.M. Norman, J.R. Mecikalski, and R.M. Aune, 1998. Agricultural Management Decisions Aids Driven by Real-Time Satellite Data. Bulletin of American Meteorological Society 79:1345-1355.

Diak, G.R., W.L. Bland, and J.R. Mecikalski, 1996. A Note on First Estimates of Surface Insolation From GOES-8 Visible Satellite Data. Agricultural and Forest Meteorology 82:219-226.

Diak, G.R. and C. Gautier, 1983. Improvements to a Simple Physical Model for Estimating Insolation From GOES Data. Journal of Climate and Applied Meteorology 22:505-508.

Duffie, J.A. and W.A. Beckman, 1980. Solar Engineering of Thermal Processes. John Wiley and Sons, New York, pp. 1-109.

Frouin, R. and B. Chertock, 1992. A Technique for Global Monitoring of net Solar Irradiance at the Ocean Surface. Part I: Model. Journal of Applied Metrology 31:1056-1066.

Frouin, R., C. Gautier, K.B. Katsaros, and J. Lind, 1988. A Comparison of Satellite and Empirical Formula Techniques for Estimating Insolation Over the Oceans. Journal of Applied Metrology 27:1016-1023.

Gautier, C., G.R. Diak, and S. Masse, 1980. A Simple Physical Model to Estimate Incident Solar Radiation at the Surface From GOES Satellite Data. Journal of Applied Metrology 19:1007-1012.

Gautier, C., G.R. Diak, and S. Masse, 1984. An Investigation of the Effects of Spatially Averaging Satellite Brightness Measurements on the Calculation of Insolation. Journal of Climate and Applied Meteorology 23:1380-1386.

Gu, J., E.A. Smith, and J.D. Merritt, 1999. Testing Energy Balance Closure With GOES-Retrieved Net Radiation and *In Situ* Measured Eddy Correlation Fluxes in BOREAS. Journal of Geophysical Research 104:27881-27893.

Hoblit, B.C., C. Castello, L. Liu, and D. Curtis, 2003. Creating a Seamless Map of Gage-Adjusted Radar Rainfall Estimates for the State of Florida. Paper presented at EWRI World Water and Environmental Congress, Philadelphia, Pennsylvania, 23-26 June.

Jacobs, J.M., M.C. Anderson, L.C. Friess, and G.R. Diak, 2004. Solar Radiation, Longwave Radiation and Emergent Wetland Evapotranspiration Estimates From Satellite Data in Florida, USA. Hydrological Sciences Journal 49:461-476.

Jacobs, J.M., D.A. Myers, M.C. Anderson, and G.R. Diak, 2002. GOES Surface Insolation to Estimate Wetlands Evapotranspiration. Journal of Hydrology 56:53-65.

Mecikalski, J.M., G.R. Diak, M.C. Anderson, and J.M. Norman, 1999. Estimating Fluxes on Continental Scales Using Remotely Sensed Data in an Atmosphere-Land Exchange Model. Journal of Applied Metrology 38:1352-1369.

Meng, C. Jesse, Rachel T. Pinker, J. Dan Tarpley, and Istvan Laszlo, 2003. A Satellite Approach for Estimating Regional Land Surface Energy Budget for GCIP/GAPP. Journal of Geophysical Research 108(D22):8861, doi: 10.1029/2002JD003088.

Monteith, J.L., 1965. Evaporation and Environment. Symposia of the Society for Experimental Biology 19:205-224.

Möser, W. and E. Raschke, 1984. Incident Solar Radiation Over Europe From METEOSAT Data. Journal of Climate and Applied Meteorology 23:166-170.

Otkin, J., M.A. Anderson, J.R. Mecikalski, and G.R. Diak, 2005. Validation of GOES-Based Insolation Estimates Using Data From the United States Climate Reference Network. Journal of Hydrometeorology 6:475-640.

Penman, H.L., 1948. Natural Evaporation From Open Water, Bare Soil and Grass. Proceedings of Royal Society London A 194, S. 120-145.

Pinker, R.T. and J.A. Ewing, 1985. Modeling Surface Solar Radiation: Model Formulation and Validation. Journal of Climate and Applied Meteorology 24:389-401.

Pinker, R.T., R. Frouin, and Z. Li, 1995. A Review of Satellite Methods to Derive Surface Shortwave Irradiance. Remote Sensing Environment 51:105-124.

Pinker, R.T. and I. Laszlo, 1992. Modeling Surface Solar Irradiance for Satellite Applications on Global Scale. Journal of Applied Metrology 31:194-211.

Pinker, R.T., J.D. Tarpley, I. Laszlo, K.E. Mitchell, P.R. Houser, E.F. Wood, J.C. Schaake, A. Robock, D. Lohmann, B.A. Cosgrove, J. Sheffield, Q. Duan, L. Luo, and R.W. Higgins, 2003. Surface Radiation Budgets in Support of the GEWEX Continental-Scale International Project (GCIP) and the GEWEX Americas Prediction Project (GAPP), Including the North American Land Data Assimilation System (NLDAS) Project. Journal of Geophysical Research 108(22):8798, doi: 10.1029/2002JDO03301.

Priestley, C.H.B. and R.J. Taylor, 1972. On the Assessment of Surface Heat Flux and Evaporation Using Large-Scale Parameters. Monthly Weather Review 100:81-92.

Raphael, C. and J.E. Hay, 1984. An Assessment of Models Which Use Satellite Data to Estimate Solar Irradiance at the Earth's Surface. Journal of Climate and Applied Meteorology 23:832-844.

Schmetz, J., 1989. Towards a Surface Radiation Climatology. Retrieval of Downward Irradiance From Satellites. Atmospheric Research 23:287-321.

Stewart, J.B., C.J. Watts, J.C. Rodriguez, H.A.R. De Bruin, A.R. van den Berg, and J. Garatuza-Payan, 1999. Use of Satellite Data to Estimate Radiation and Evaporation for Northwest Mexico. Agriculture and Water Management 38:181-193.

Tarpley, J.D., 1979. Estimating Incident Solar Radiation at the Surface From Geostationary Satellite Data. Journal of Applied Meteorology 18:1172-1181.

Weymouth, G. and J. LeMarshall, 1999. An Operational System to Estimate Global Solar Exposure Over the Australian Region From Satellite Observations. Australian Meteorological Magazine 48:181-195.